

Supporting Information

Self-Healing Polyacrylate Coatings with Dynamic H-Bonds Between Urea Groups

Marie Mottoul,^{1,3} Sylvain Giljean,² Marie-José Pac,² Véronic Landry³ and Jean-François Morin*,¹

¹ Département de chimie and Centre de Recherche sur les Matériaux Avancés

(CERMA), 1045 Ave de la Médecine, Université Laval, Québec, Canada G1V 0A6

² Université de Haute-Alsace, Laboratoire de Physique et Mécanique Textiles (UR 4365), 68093 Mulhouse, France

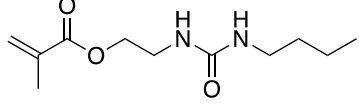
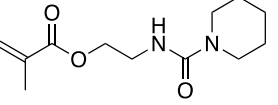
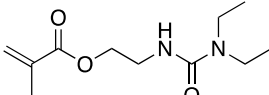
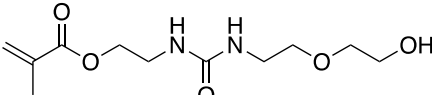
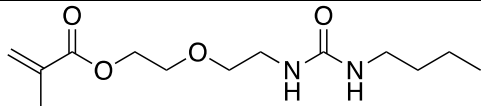
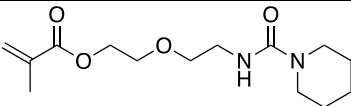
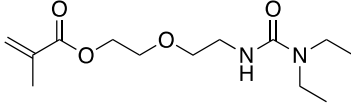
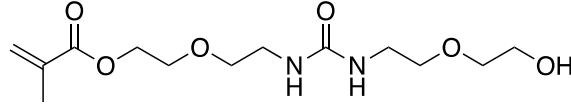
³ NSERC-Canlak industrial Research Chair in Interior Wood Product Finishes and Centre de Recherche sur les Matériaux Renouvelables (CRMR), Département des sciences du bois et de la forêt, 2425 rue de la Terrasse, Université Laval, Québec, Canada G1V 0A6

Corresponding author: jean-francois.morin@chm.ulaval.ca

TABLE OF CONTENT

1. STRUCTURES AND ABBREVIATIONS OF THE MONOMERS	3
2. MEASURED GLOSS VALUES AND SCRATCH DEPTH VALUES	4
3. CHARACTERIZATION OF THE MONOMERS	4
A₁-Bu	4
A₁-Pi	6
A₁-Di	7
A₁-EE	9
A₂-Bu	10
A₂-Pi	12
A₂-Di	13
A₂-EE	15
4. CHARACTERIZATION OF THE POLYMERS	17
PA₀	17
PA₁-Bu	18
PA₁-Pi	20
PA₁-Di	21
PA₁-EE	23
PA₂-Bu	24
PA₂-Pi	26
PA₂-Di	27
PA₂-EE	29

1. Structures and abbreviations of the monomers

 A1-Bu	 A1-Pi
 A1-Di	 A1-EE
 A2-Bu	 A2-Pi
 A2-Di	 A2-EE

2. Measured gloss values and scratch depth values

Table S1: Table of the gloss values of the virgin samples (g_{virgin}), after abrasion (g_{damaged}) and after healing (g_{healed}) and highest scratch depth values observed.

	g_{virgin}	g_{damaged}	g_{healed}	Highest scratch depth values (μm)
PA₀	133	85.5	135	11
PA₁-Pi	74.5	19.7	48.5	6
PA₁-Di	125	25.9	80.7	7
PA₁-Bu	47.1	9.6	23.9	10
PA₁-EE	125	28.5	133	8
PA₂-Pi	111	29.1	105	8
PA₂-Di	118	76.8	123	10
PA₂-Bu	87.3	11.0	54.4	7
PA₂-EE	98.8	66.1	101	4

Some gloss values after healing are slightly higher than the values of the virgin sample due to small defects of the coating that were corrected through self-healing.

3. Characterization of the monomers

A₁-Bu

A₁-Bu: ^1H NMR (500 MHz, CDCl₃): δ 6.14 – 6.13 (m, 1H), 5.61 (p, J = 1.6 Hz, 1H), 4.26 (t, 2H), 3.52 (t, J = 5.4 Hz, 2H), 3.17 (t, J = 7.1 Hz, 2H), 1.96 (dd, J = 1.6, 1.0 Hz, 3H), 1.53 – 1.46 (m, 2H), 1.41 – 1.32 (m, 2H), 0.93 (t, J = 7.3 Hz, 3H). ^{13}C NMR (126 MHz, CDCl₃): δ 167.6, 136.0, 126.0, 64.2, 40.3, 39.6, 32.2, 20.0, 18.3, 13.8, 13.8. HRMS (ESI+): calcd for C₁₁H₂₁N₂O₃ [M+H]⁺ 229.1552 u, found 229.1547 u

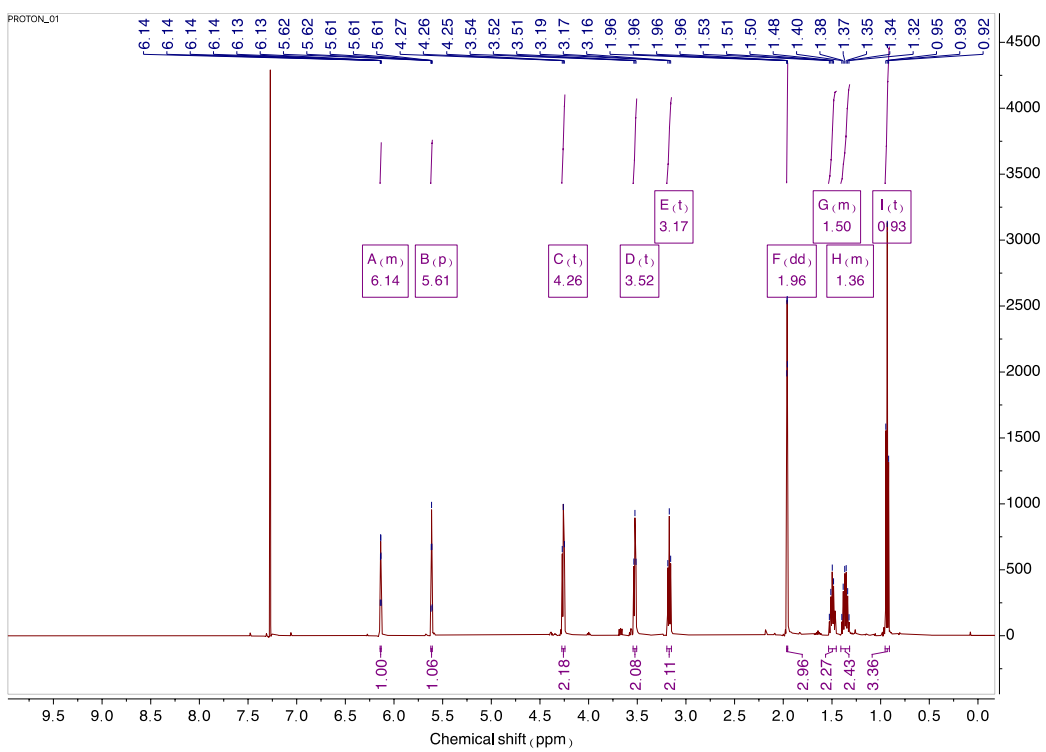


Figure S1 : ^1H NMR spectrum of the **A1-Bu** in CDCl_3 .

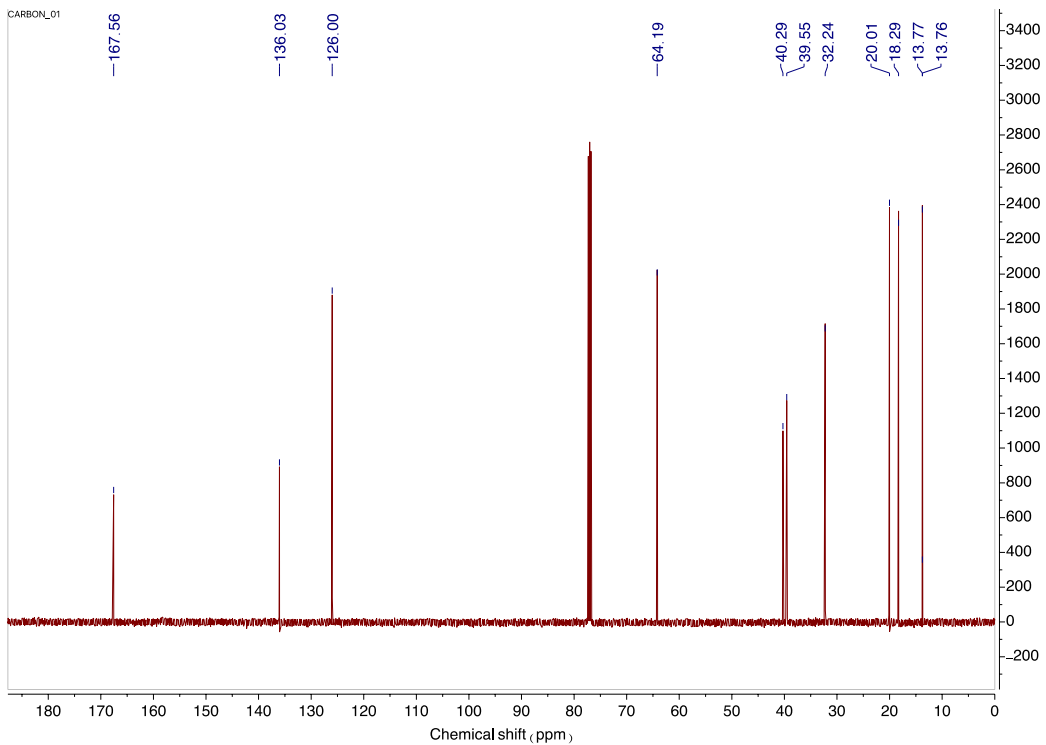


Figure S2 : ^{31}C NMR spectrum of the **A1-Bu** in CDCl_3 .

A1-Pi

A1-Pi: ^1H NMR (500 MHz, CDCl_3): δ 6.06 – 6.04 (m, 1H), 5.52 (p, $J = 1.6$ Hz, 1H), 4.98 (s, 1H), 4.22 – 4.18 (m, 2H), 3.47 (q, $J = 4.7$ Hz, 2H), 3.26 – 3.19 (m, 4H), 1.87 (dd, $J = 1.6, 1.0$ Hz, 3H), 1.55 – 1.46 (m, 7H). ^{13}C NMR (126 MHz, CDCl_3): δ 167.7, 157.3, 136.1, 126.0, 64.1, 45.0, 40.4, 25.5, 24.3, 18.4. HRMS (ESI+): calcd for $\text{C}_{12}\text{H}_{21}\text{N}_2\text{O}_3$ [$\text{M}+\text{H}]^+$ 241.1552 u, found 241.1547 u

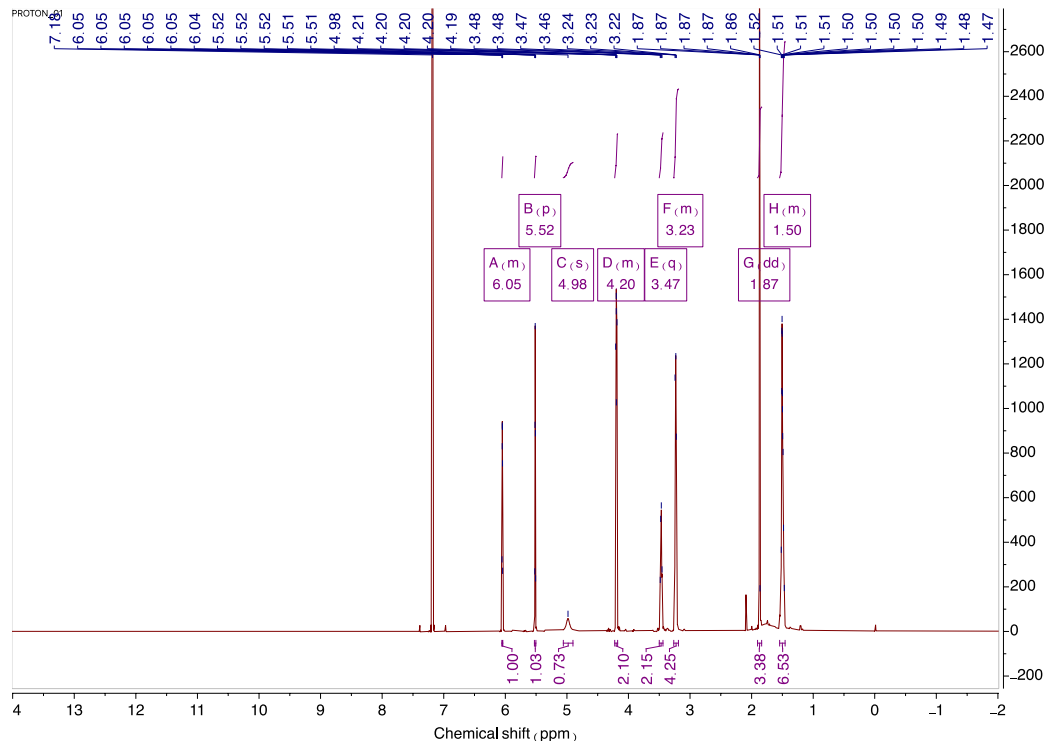


Figure S3 : ^1H NMR spectrum of the **A1-Pi** in CDCl_3 .

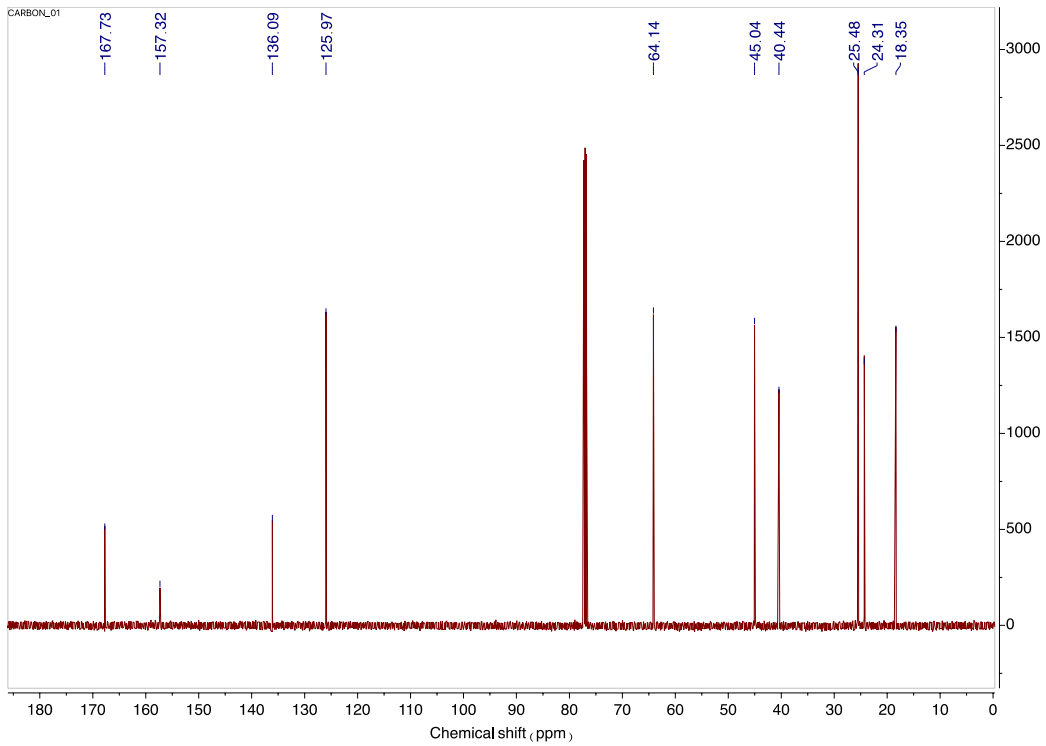


Figure S4 : ^{13}C NMR spectrum of the **A1-Pi** in CDCl_3 .

A1-Di

A1-Di: ^1H NMR (500 MHz, CDCl_3): δ 6.12 – 6.10 (m, 1H), 5.58 (p, $J = 1.6$ Hz, 1H), 4.89 (s, 1H), 4.29 – 4.25 (m, 2H), 3.53 (t, $J = 5.4$ Hz, 2H), 3.24 (q, $J = 7.1$ Hz, 4H), 1.93 (dd, $J = 1.6, 1.0$ Hz, 3H), 1.12 (t, $J = 7.1$ Hz, 6H). ^{13}C NMR (126 MHz, CDCl_3): δ 167.4, 157.1, 136.0, 125.6, 64.0, 41.00, 40.0, 18.2, 13.6. HRMS (ESI+): calcd for $\text{C}_{11}\text{H}_{21}\text{N}_2\text{O}_3$ [$\text{M}+\text{H}$] $^+$ 229.1552 u, found 229.1547 u

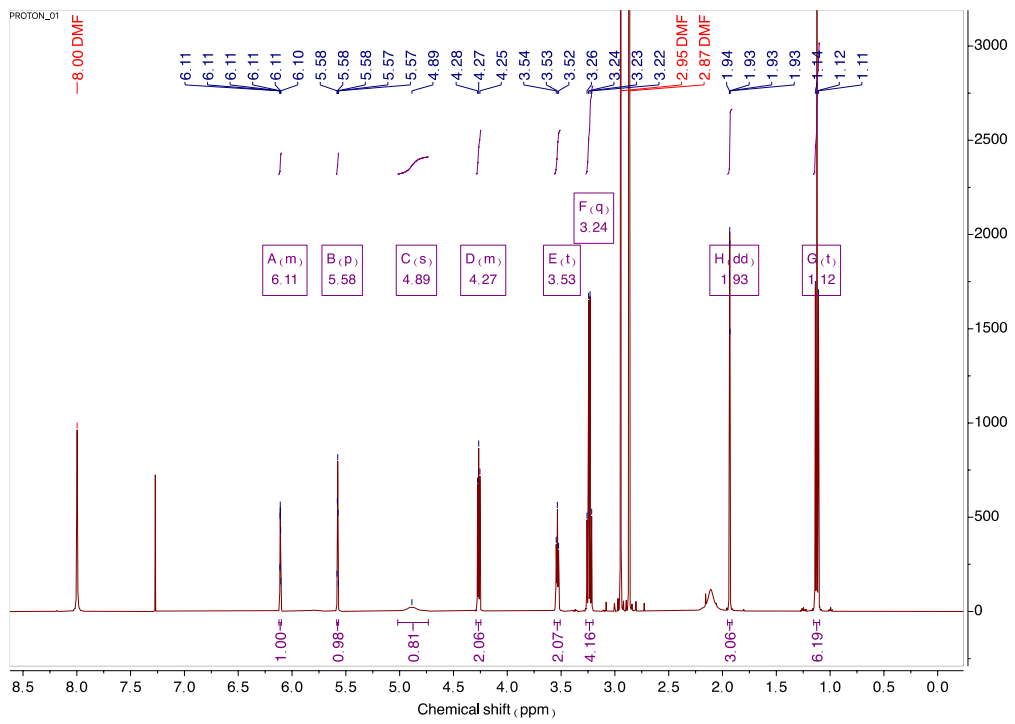


Figure S5: ^1H NMR spectrum of the crude of **A1-Di** in CDCl_3 .

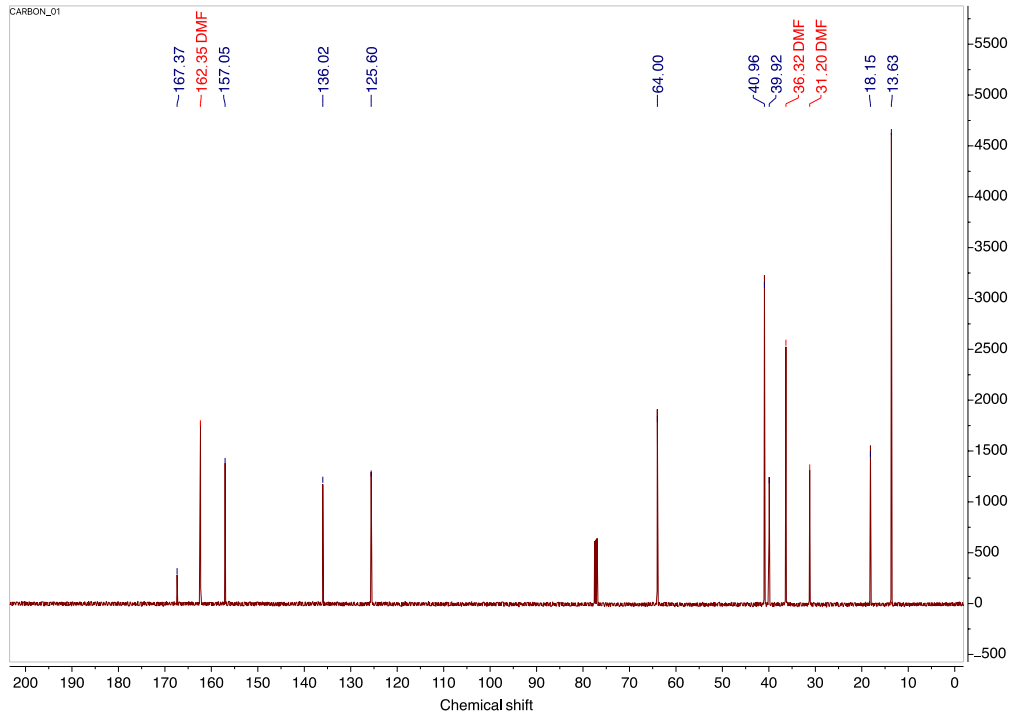


Figure S6 : ^{13}C NMR spectrum of the crude of **A1-Di** in CDCl_3 .

A1-EE

A1-EE: ^1H NMR (500 MHz, CDCl_3): δ 6.14 – 6.11 (m, 1H), 5.61 – 5.57 (m, 1H), 4.21 (q, $J = 5.7$ Hz, 2H), 3.73 (q, $J = 4.8$ Hz, 2H), 3.59 – 3.53 (m, 4H), 3.51 – 3.46 (m, 2H), 3.38 (q, $J = 5.2$ Hz, 2H), 1.95 – 1.92 (m, 3H). ^{13}C NMR (126 MHz, CDCl_3): δ 167.4, 158.9, 136.1, 125.7, 72.2, 70.5, 64.3, 61.4, 40.0, 39.0, 18.2. HRMS (ESI+): calcd for $\text{C}_{11}\text{H}_{21}\text{N}_2\text{O}_5$ [$\text{M}+\text{H}]^+$ 261.1450 u, found 261.1445 u

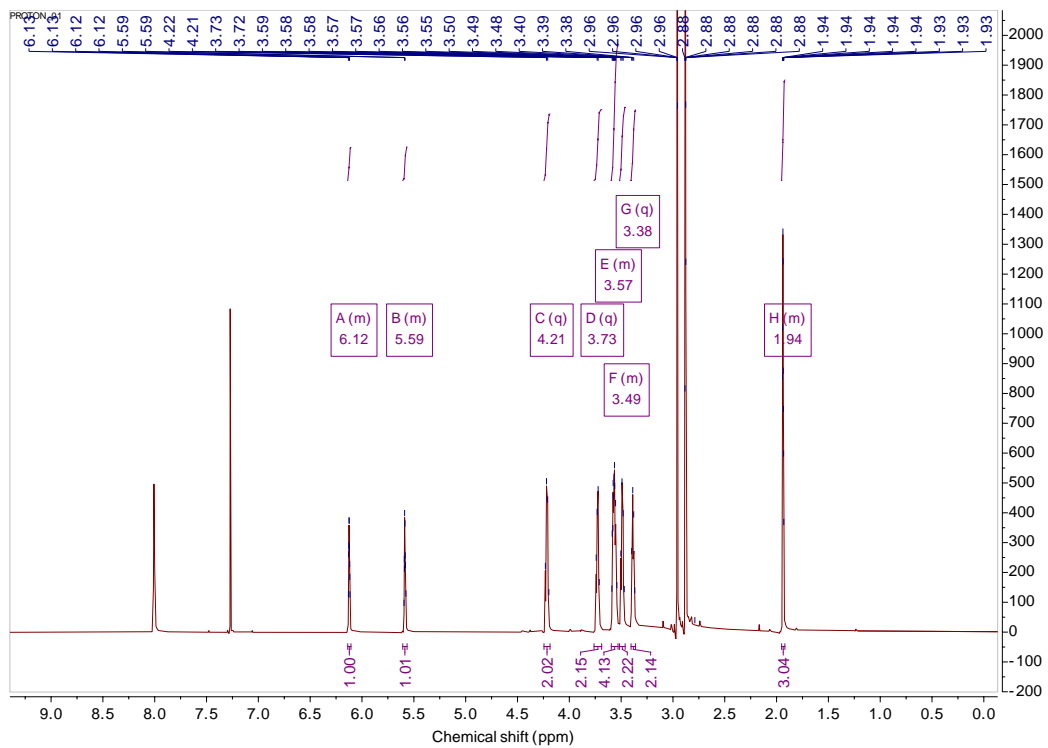


Figure S7 : ^1H NMR spectrum of **A1-EE** in CDCl_3 .

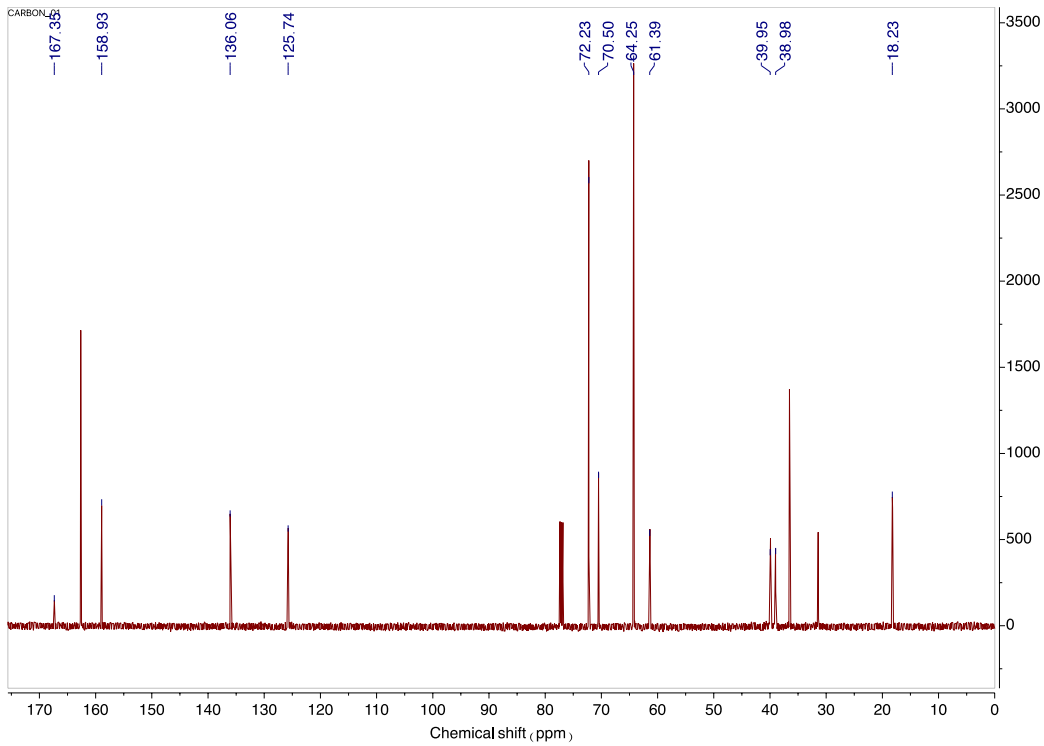


Figure S8 : ^{13}C NMR spectrum of **A1-EE** in CDCl_3 .

A₂-Bu

A₂-Bu: ^1H NMR (500 MHz, CDCl_3): $\delta_{\text{H}} = 6.14$ (dq, $J = 2.0, 1.1$ Hz, 1H), 5.61 (p, $J = 1.6$ Hz, 1H), 4.34 – 4.30 (m, 2H), 3.74 – 3.71 (m, 2H), 3.60 – 3.56 (m, 2H), 3.38 (dd, $J = 5.6, 4.4$ Hz, 2H), 3.16 (dd, $J = 8.0, 6.2$ Hz, 2H), 1.96 (dd, $J = 1.6, 1.0$ Hz, 3H), 1.51 – 1.44 (m, 2H), 1.40 – 1.30 (m, 3H), 0.92 (t, $J = 7.3$ Hz, 3H). Two H are not observed. ^{13}C NMR (126 MHz, CDCl_3): $\delta_{\text{C}} = 167.5, 158.7, 136.1, 126.0, 71.0, 69.0, 63.7, 40.4, 40.3, 32.2, 20.0, 18.3, 13.8$. HRMS (ESI+): calcd for $\text{C}_{13}\text{H}_{25}\text{N}_2\text{O}_4$ $[\text{M}+\text{H}]^+$ 273.1814 u, found 273.1809 u

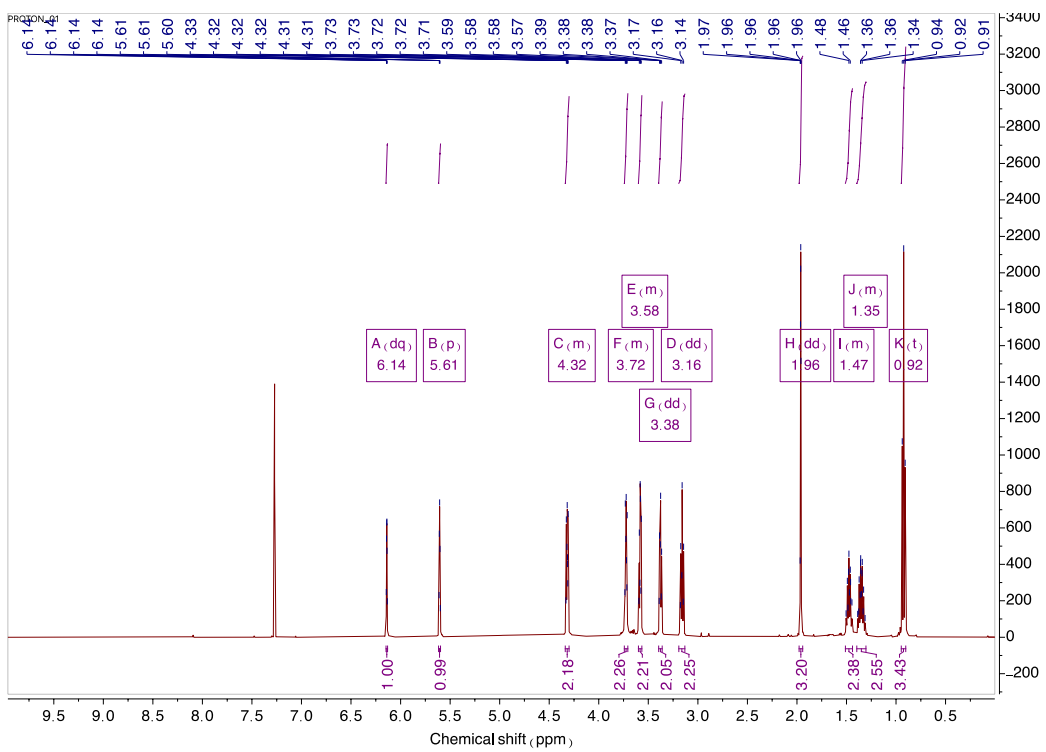


Figure S9 : ^1H NMR spectrum of **A₂-Bu** in CDCl_3

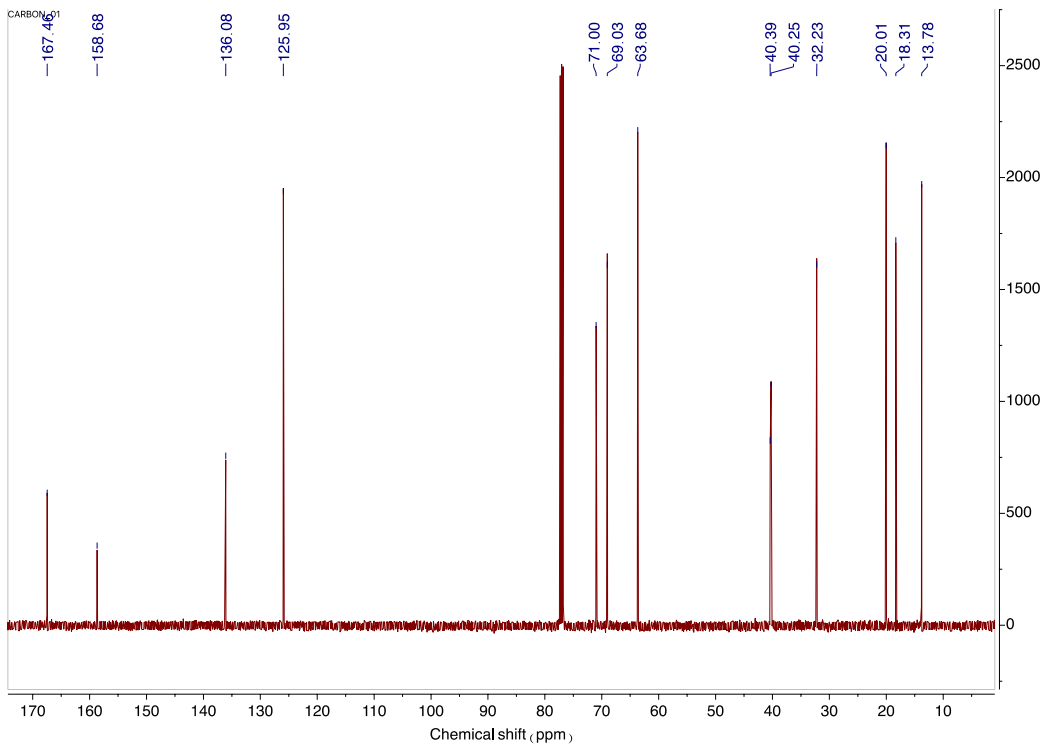


Figure S10 : ^{13}C NMR spectrum of **A₂-Bu** in CDCl_3 .

A₂-Pi

A₂-Pi: ¹H NMR (500 MHz, CDCl₃): δ 6.12 – 6.10 (m, 1H), 5.57 (p, *J* = 1.6 Hz, 1H), 4.31 – 4.28 (m, 2H), 3.72 – 3.69 (m, 2H), 3.59 – 3.55 (m, 2H), 3.44 – 3.40 (m, 2H), 3.33 – 3.28 (m, 4H), 1.94 (dd, *J* = 1.6, 1.0 Hz, 3H), 1.61 – 1.51 (m, 6H). ¹³C NMR (126 MHz, CDCl₃): δ 167.1, 157.6, 136.0, 125.6, 77.5, 77.3, 77.0, 70.3, 68.7, 63.6, 44.6, 40.4, 25.5, 24.3, 18.1. HRMS (ESI+): calcd for C₁₄H₂₅N₂O₄ [M+H]⁺ 285.1814 u, found 285.1809 u

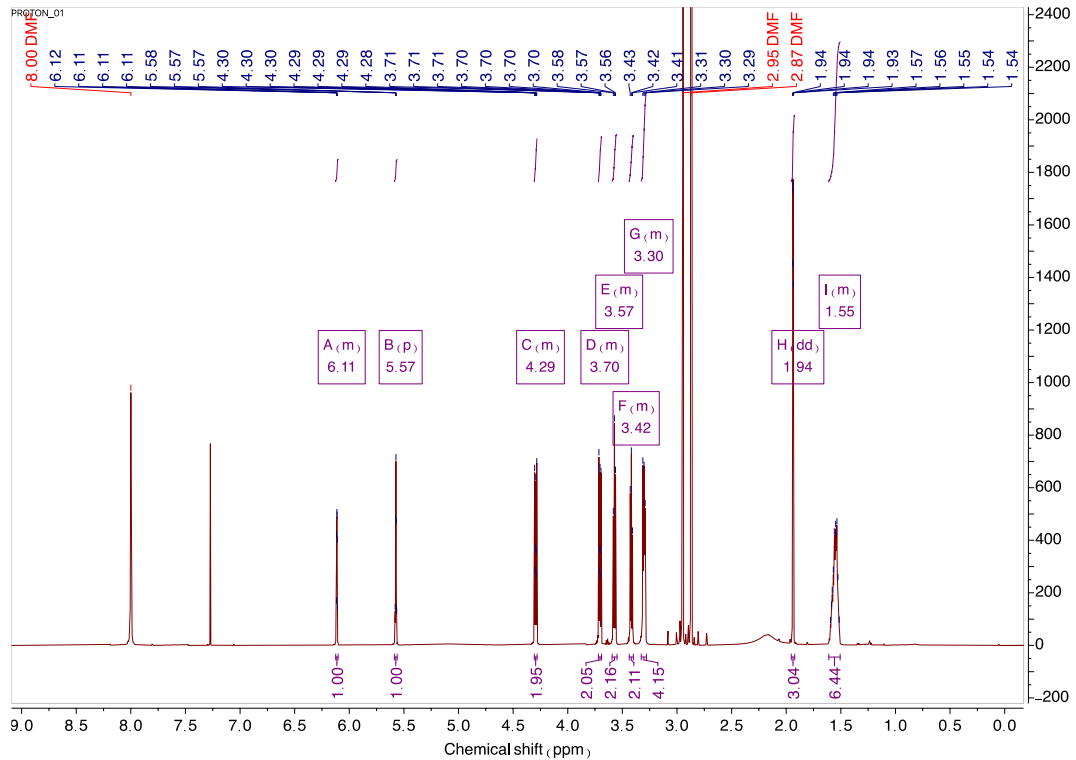


Figure S11: ¹H NMR spectrum of A₂-Pi in CDCl₃.

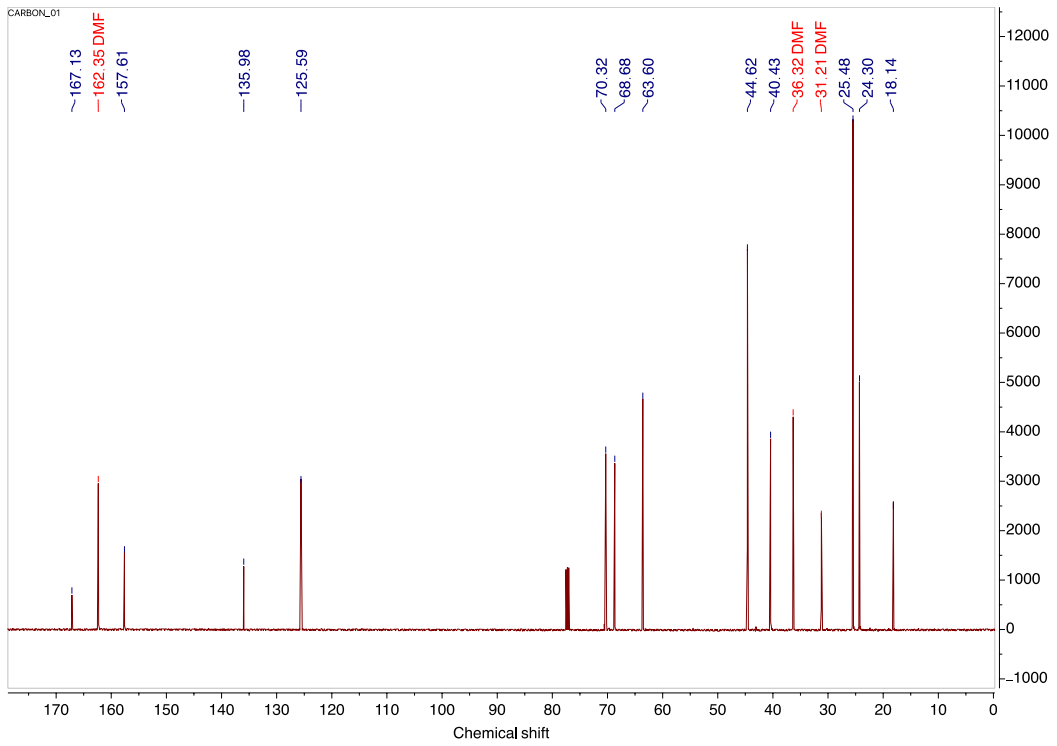


Figure S12: ^{13}C NMR spectrum of the crude of **A2-Pi** synthesis in CDCl_3 .

A2-Di

A2-Di: ^1H NMR (500 MHz, CDCl_3): δ 6.11 – 6.09 (m, 1H), 5.58 – 5.55 (m, 1H), 4.30 – 4.26 (m, 2H), 3.72 – 3.68 (m, 2H), 3.59 – 3.54 (m, 2H), 3.42 (q, $J = 4.7$ Hz, 2H), 3.27 – 3.20 (m, 4H), 1.95 – 1.91 (m, 3H), 1.14 – 1.09 (m, 6H). ^{13}C NMR (126 MHz, CDCl_3): δ 167.1, 157.2, 136.0, 125.6, 70.4, 68.7, 63.7, 40.9, 40.3, 18.1, 13.7. HRMS (ESI+): calcd for $\text{C}_{13}\text{H}_{25}\text{N}_2\text{O}_4$ [$\text{M}+\text{H}]^+$ 273.1814 u, found 273.1809 u

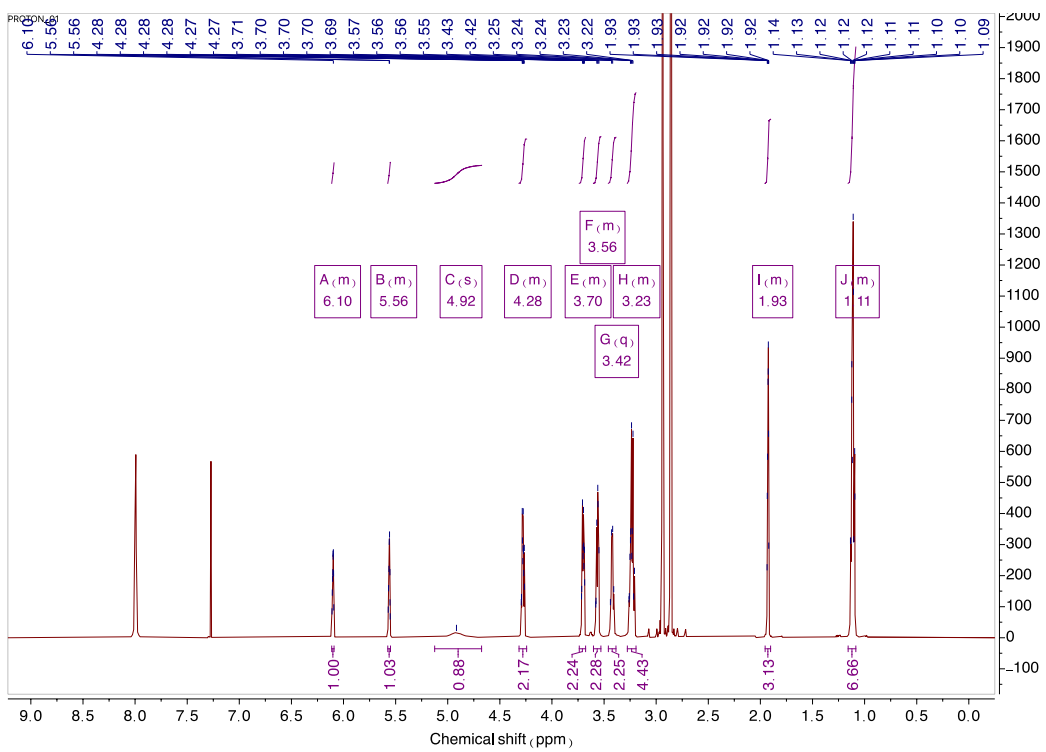


Figure S13: ^1H NMR spectrum of **A₂-Di** in CDCl_3 .

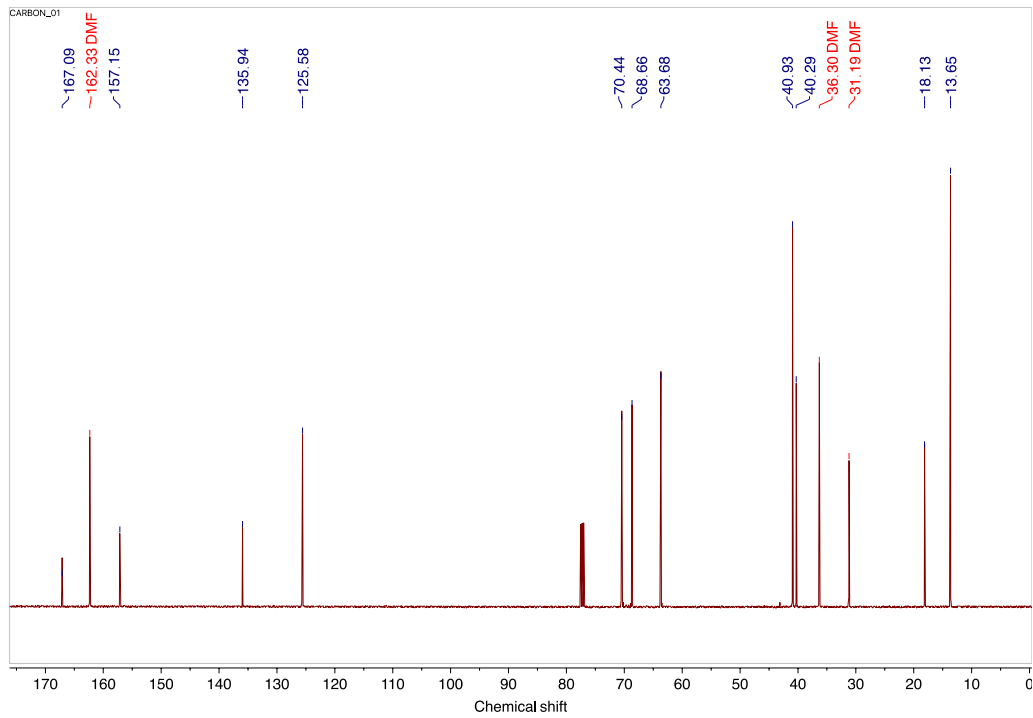


Figure S14: ^{13}C NMR spectrum of **A₂-Di** in CDCl_3 .

A₂-EE

A₂-EE: ¹H NMR (500 MHz, CDCl₃): δ 6.12 – 6.10 (m, 1H), 5.59 – 5.56 (m, 1H), 4.30 – 4.25 (m, 2H), 3.72 – 3.67 (m, 4H), 3.57 – 3.52 (m, 6H), 3.37 – 3.33 (m, 4H), 1.94 – 1.92 (m, 3H). ¹³C NMR (126 MHz, CDCl₃): δ 167.2, 159.0, 135.9, 125.8, 72.2, 70.8, 70.5, 68.6, 63.7, 61.2, 39.8, 39.8, 18.1. HRMS (ESI+): calcd for C₁₃H₂₅N₂O₆ [M+H]⁺ 305.1713 u, found 305.1707 u

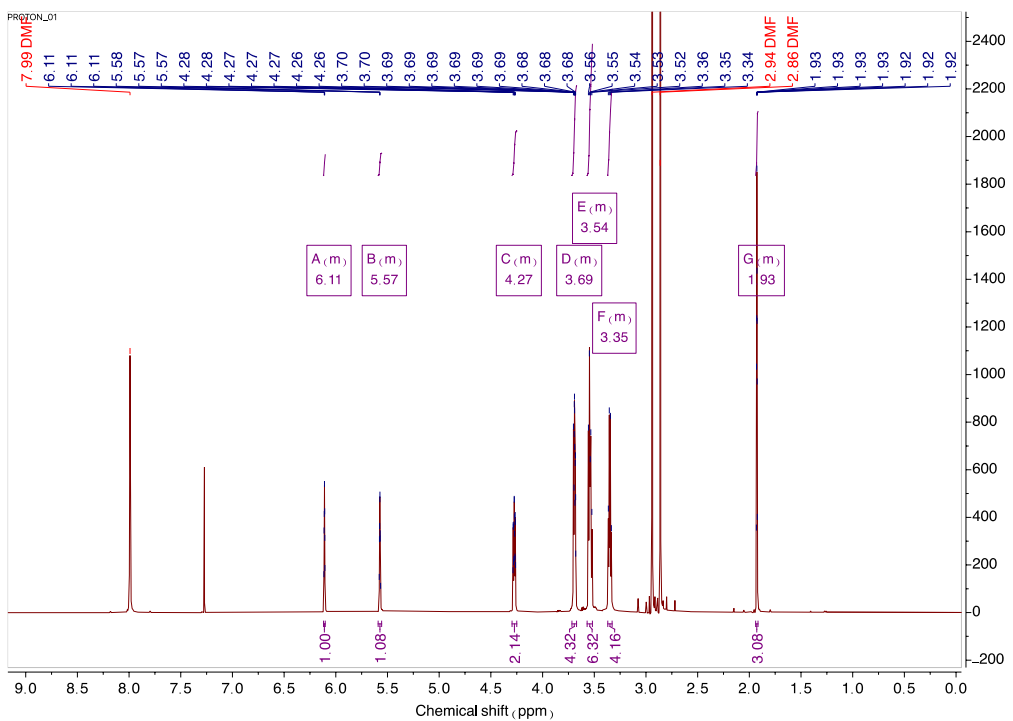


Figure S15: ¹H NMR spectrum of A₂-EE in CDCl₃.

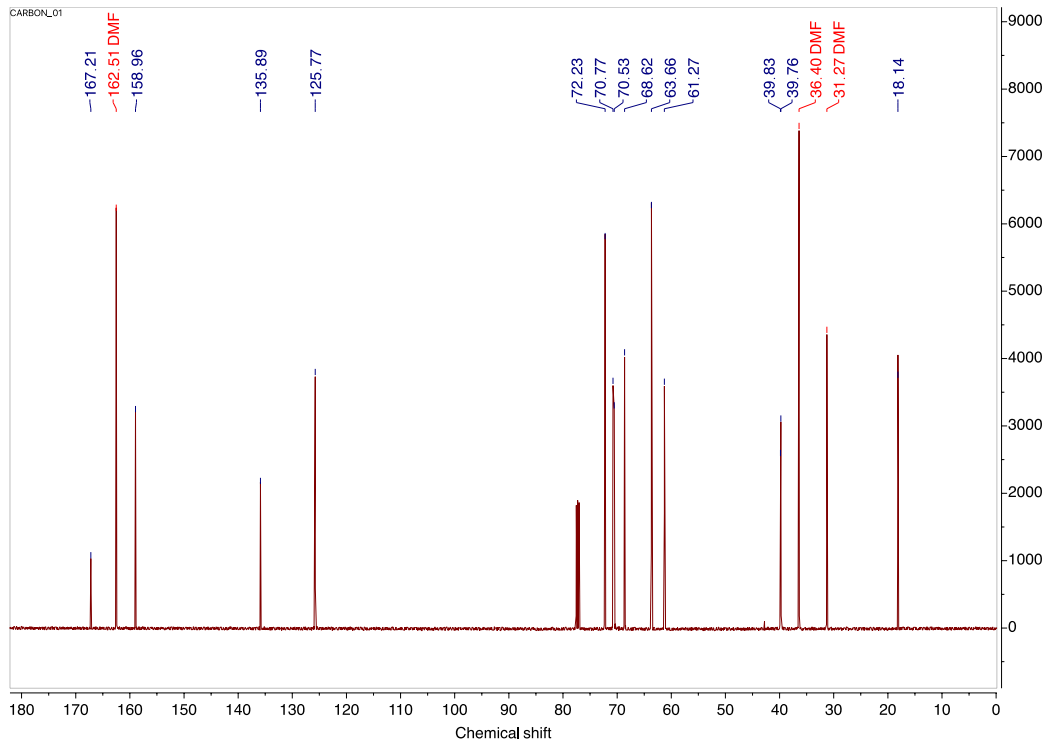


Figure S16: ^{13}C NMR spectrum of **A₂-EE** in CDCl_3

4. Characterization of the polymers

PA₀

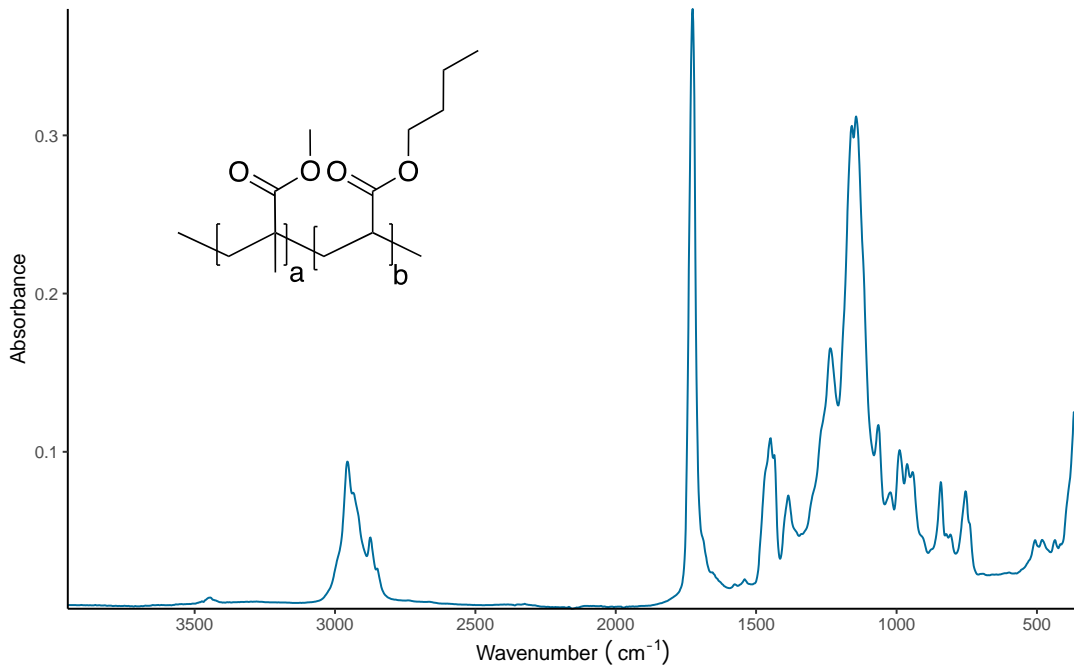


Figure S17: IR spectrum of **PA₀**.

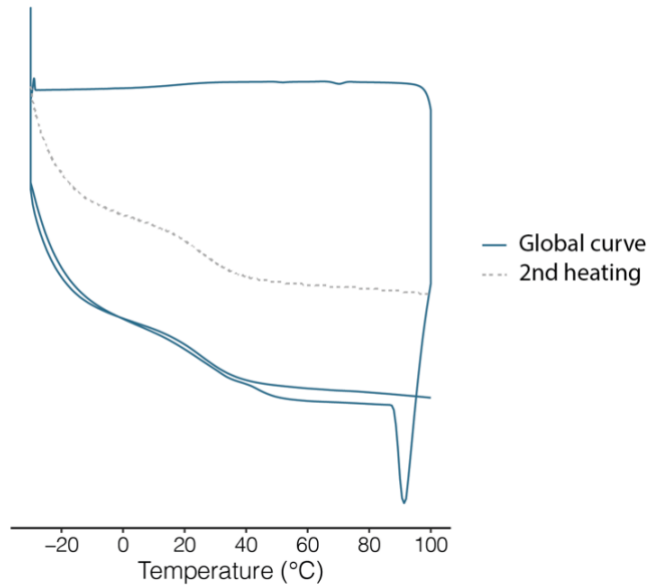


Figure S18: DSC thermogram of **PA₀** ($T_g = 26$ °C).

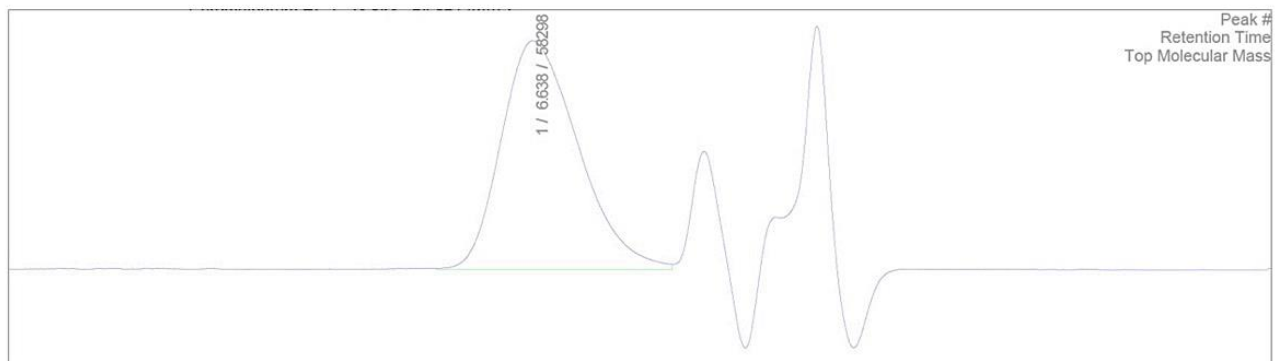


Figure S19: SEC traces of **PA₀** polymer ($M_n = 24\,000$ g/mol, $M_w = 64\,100$ g/mol, $D = 2.7$)

PA_{1-Bu}

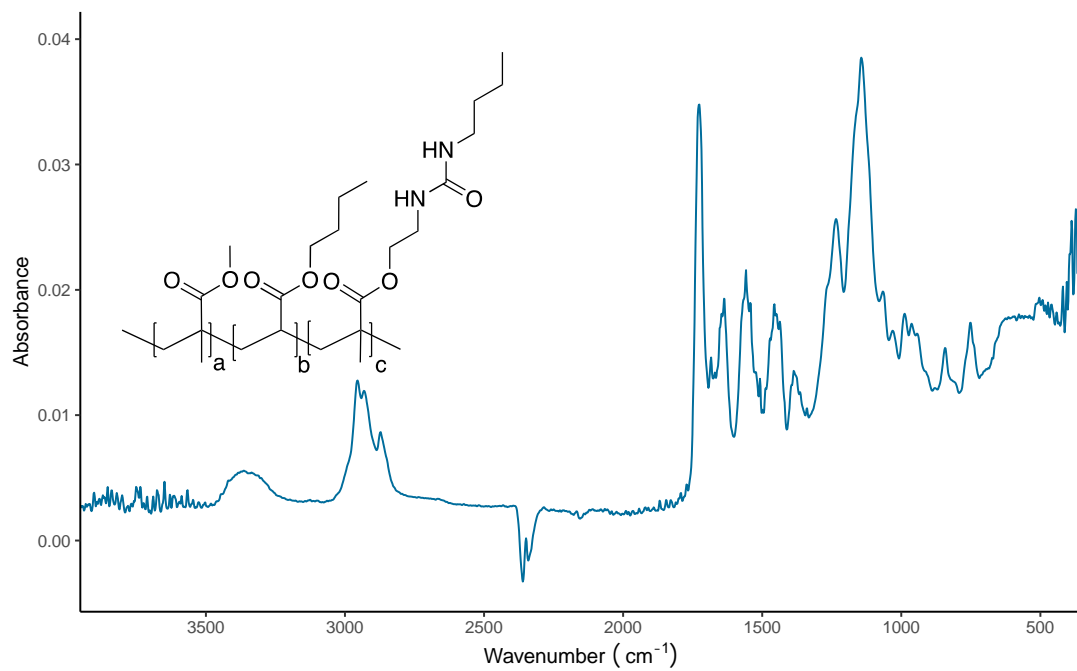


Figure S20: IR spectrum of **PA_{1-Bu}**.

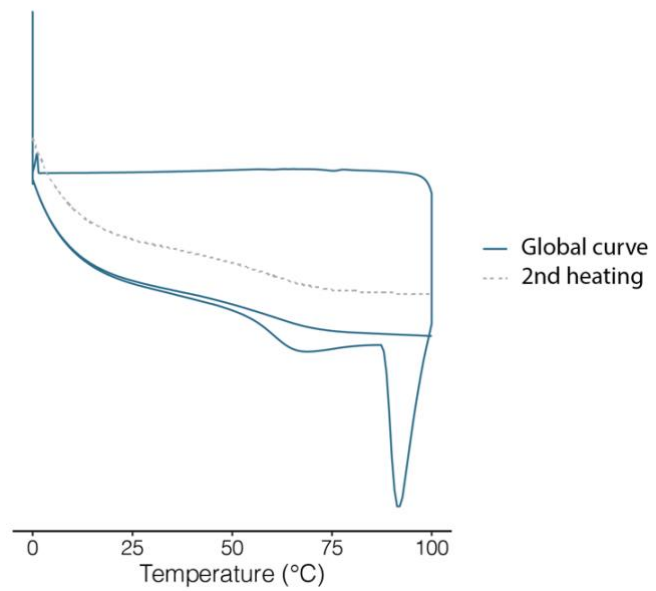


Figure S21: DSC thermogram of **PA₁-Bu** ($T_g = 54$ °C).

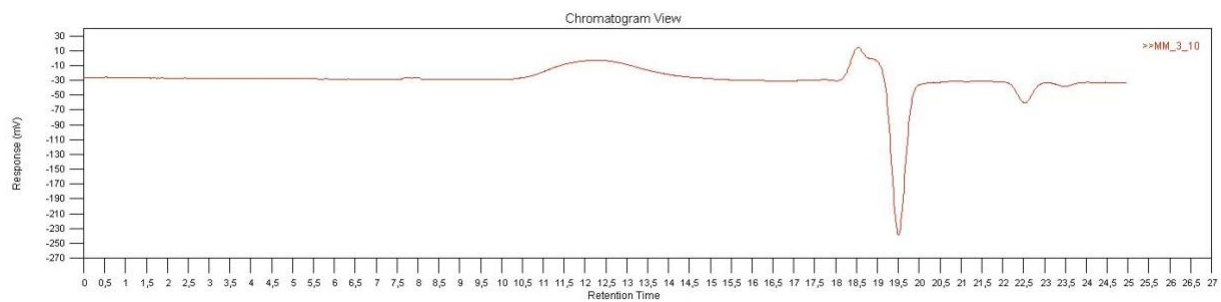


Figure S22: SEC traces of **PA₁-Bu** ($M_n = 143\,000$ g/mol, $M_w = 362\,000$ g/mol, $D = 2.5$)

PA₁-Pi

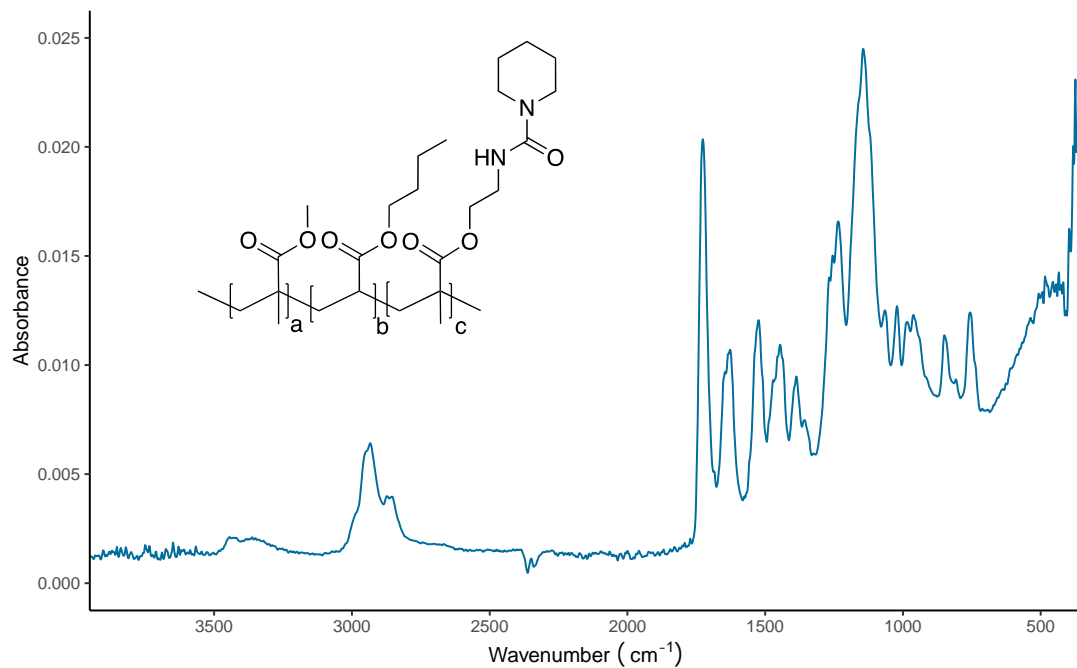


Figure S23: IR spectrum of **PA₁-Pi**.

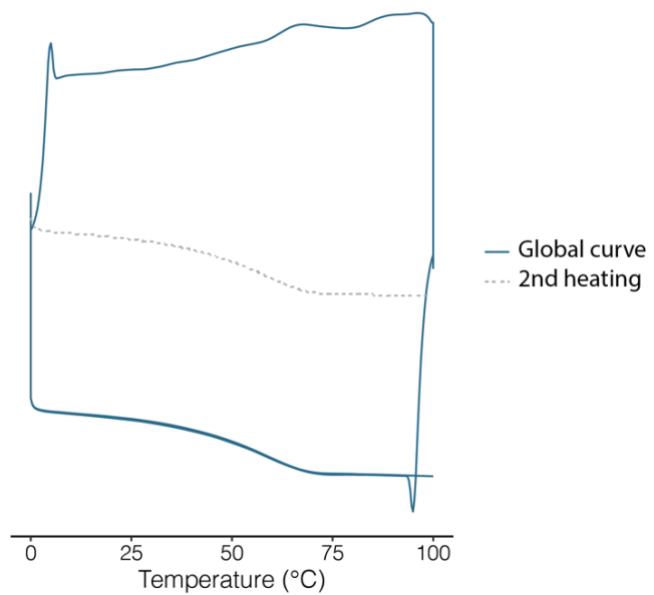


Figure S24: DSC thermogram of **PA₁-Pi** ($T_g = 57$ °C).

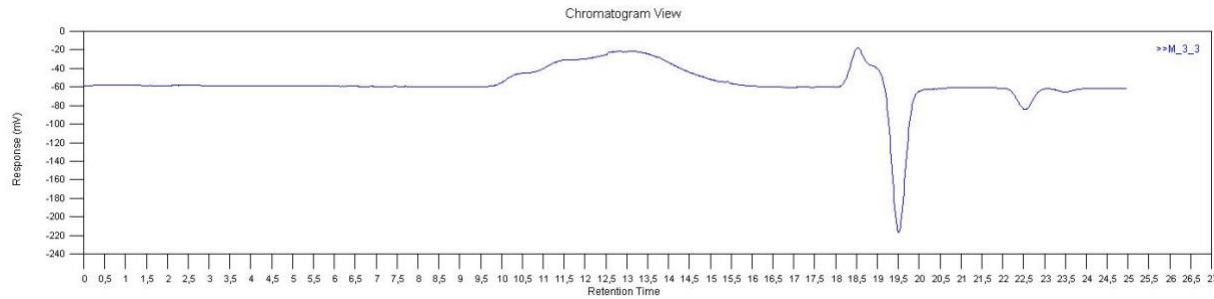


Figure S25: SEC traces of of **PA1-Pi** ($M_n = 81\ 500\ \text{g/mol}$, $M_w = 406\ 600\ \text{g/mol}$, $D = 5.0$)

PA1-Di

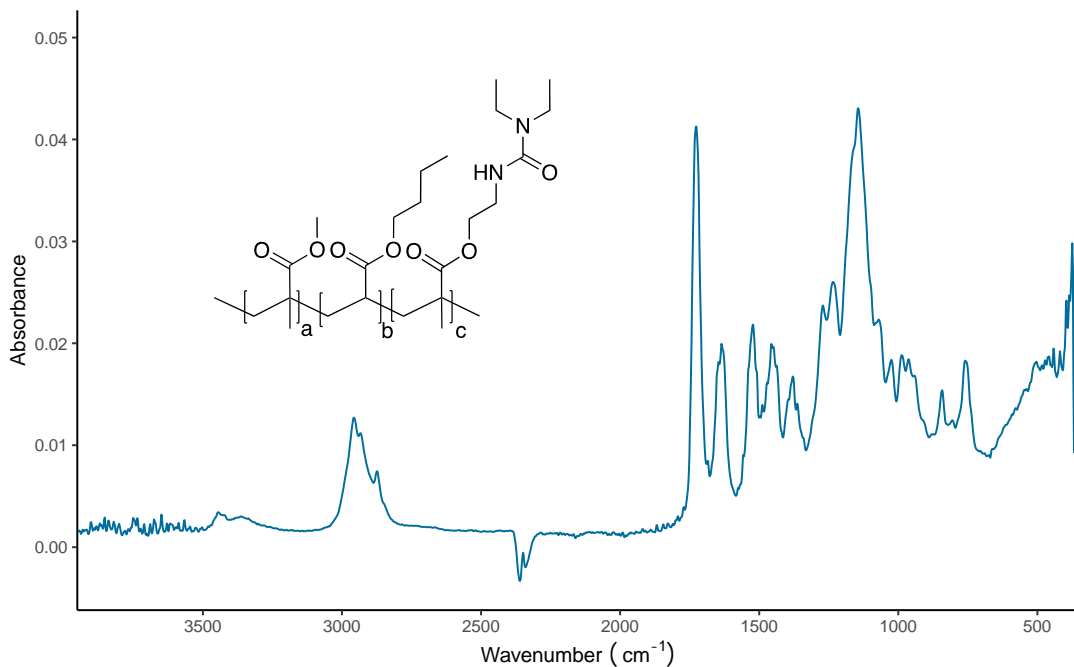


Figure S26: IR spectrum of **PA1-Di**.

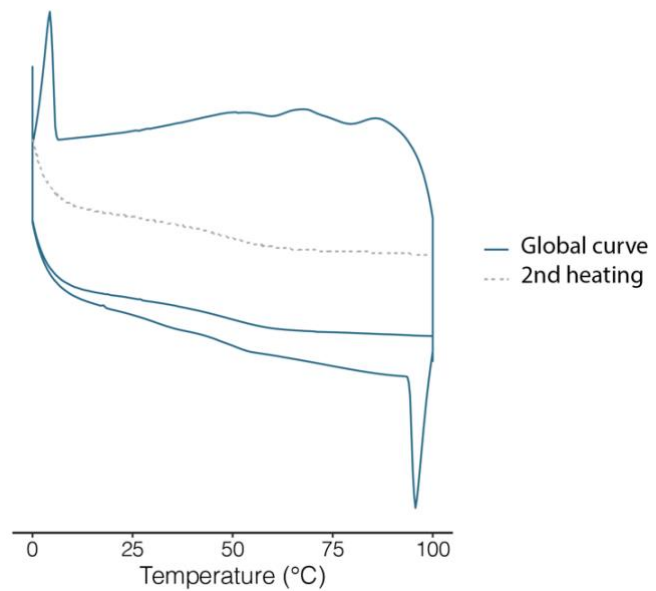


Figure S27: DSC thermogram of of **PA1-Di** ($T_g = 51 \text{ } ^\circ\text{C}$).

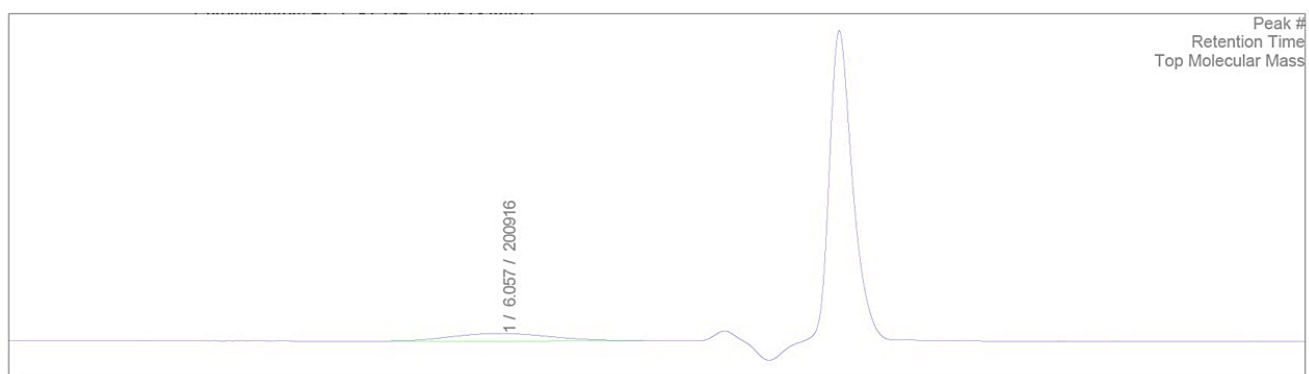


Figure S28: SEC traces of **PA1-Di** ($M_n = 88\,600 \text{ g/mol}$, $M_w = 352\,400 \text{ g/mol}$, $D = 4.0$)

PA1-EE

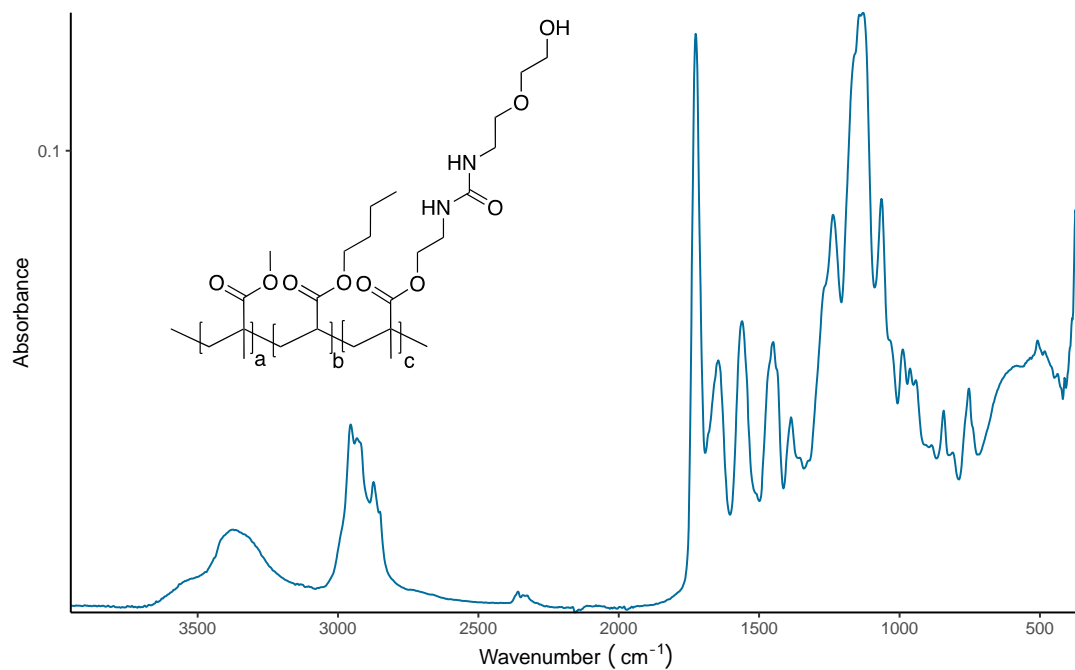


Figure S29: IR spectrum of **PA1-EE**.

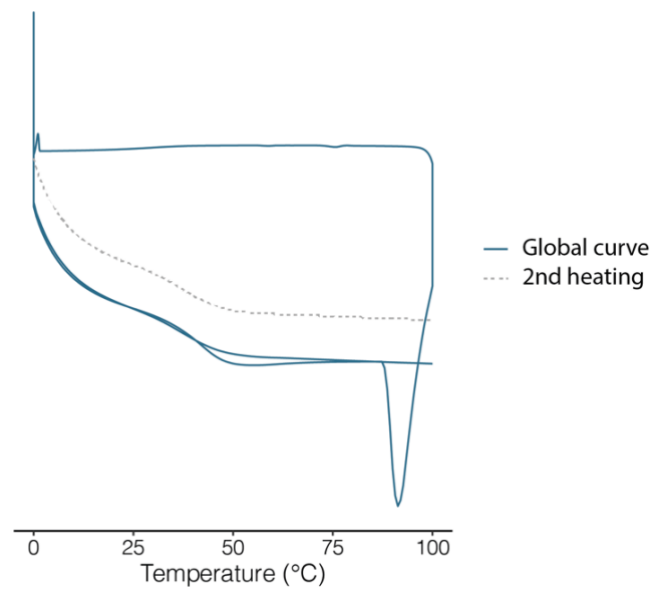


Figure S30: DSC thermogram of **PA1-EE** ($T_g = 39 \text{ }^{\circ}\text{C}$).

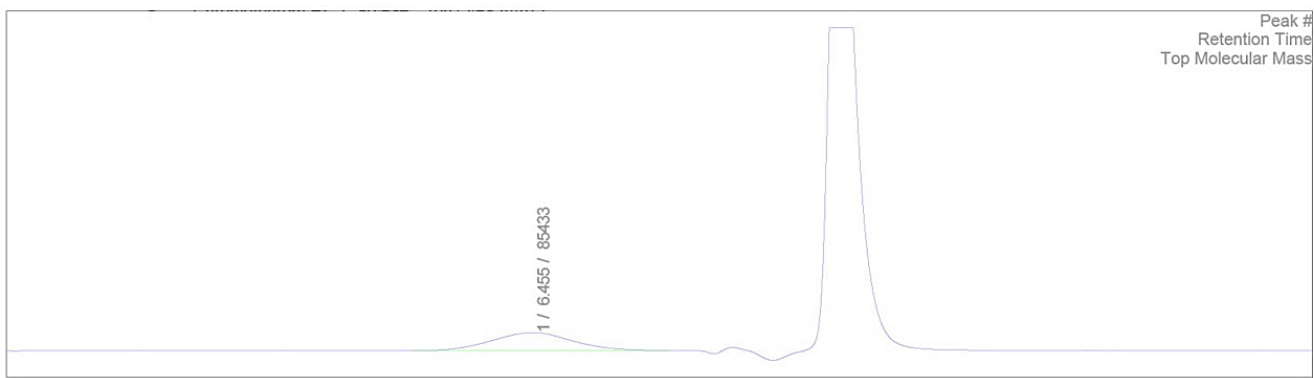


Figure S31: SEC traces of **PA₁-EE** ($M_n = 50\ 800\ \text{g/mol}$, $M_w = 144\ 700\ \text{g/mol}$, $D = 2.9$)

PA₂-Bu

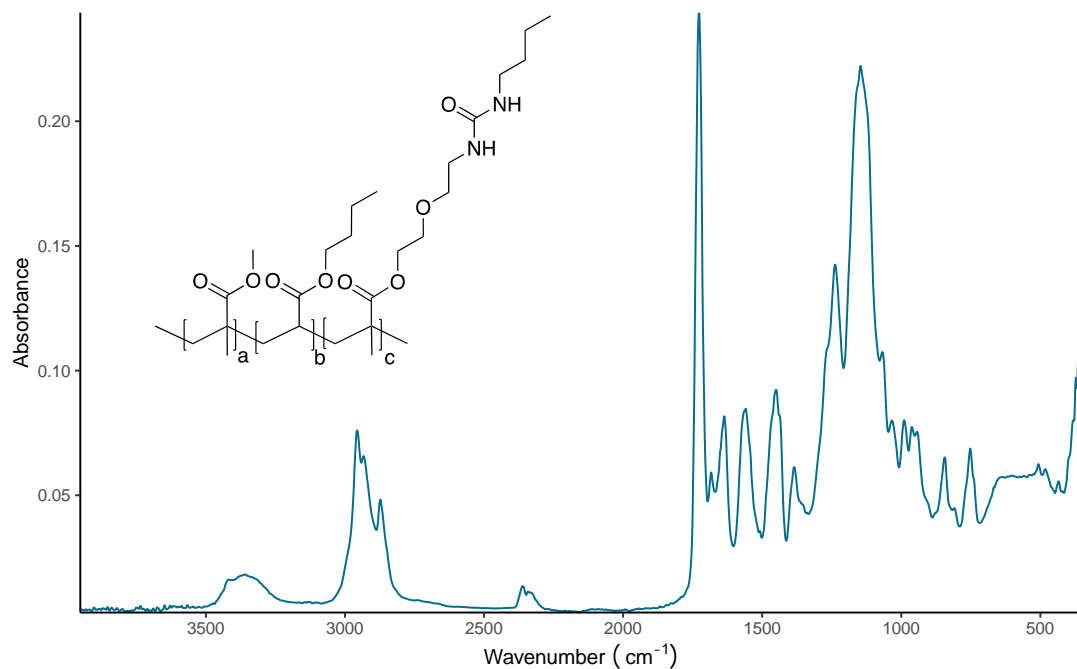


Figure S32: IR spectrum of **PA₂-Bu**.

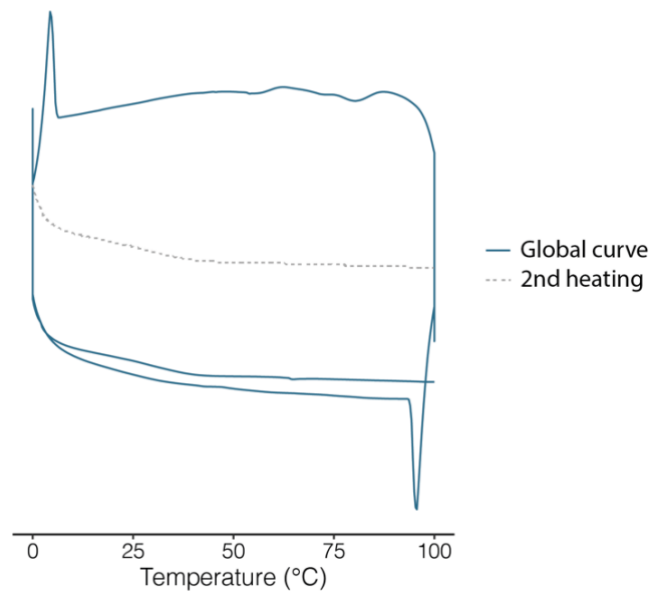


Figure S33: DSC thermogram of **PA₂-Bu** ($T_g = 30$ °C).

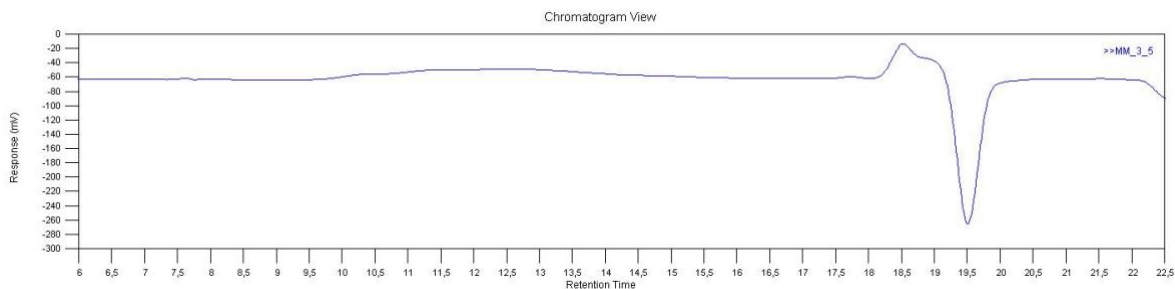


Figure S34: SEC traces of **PA₂-Bu** ($M_n = 103\,300$ g/mol, $M_w = 548\,000$ g/mol, $D = 5.3$)

PA₂-Pi

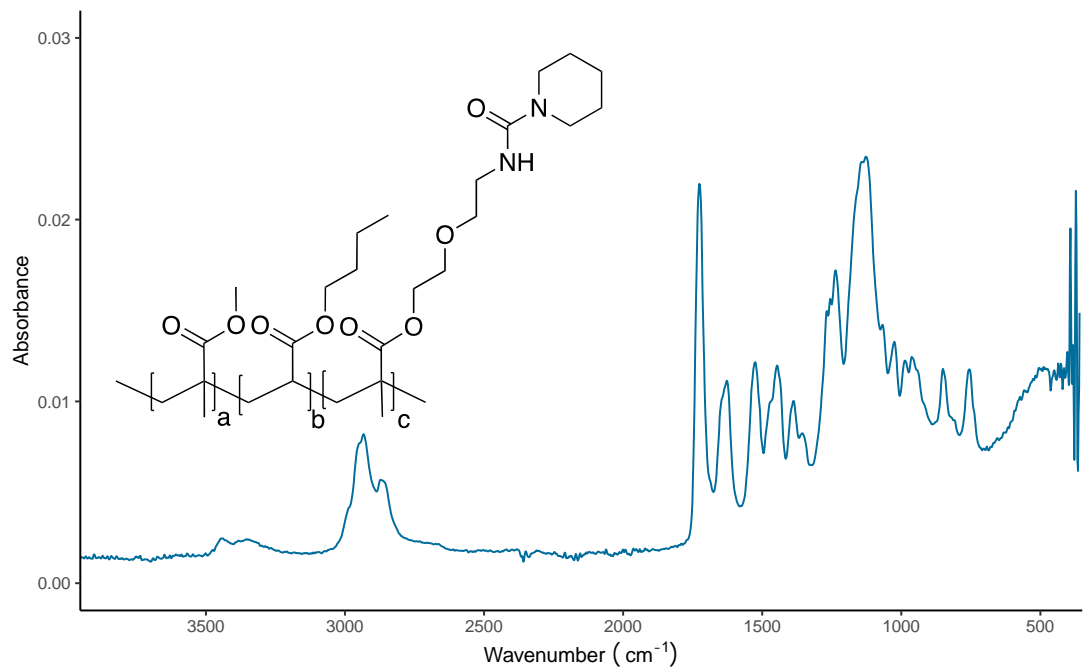


Figure S35: IR spectrum of **PA₂-Pi**.

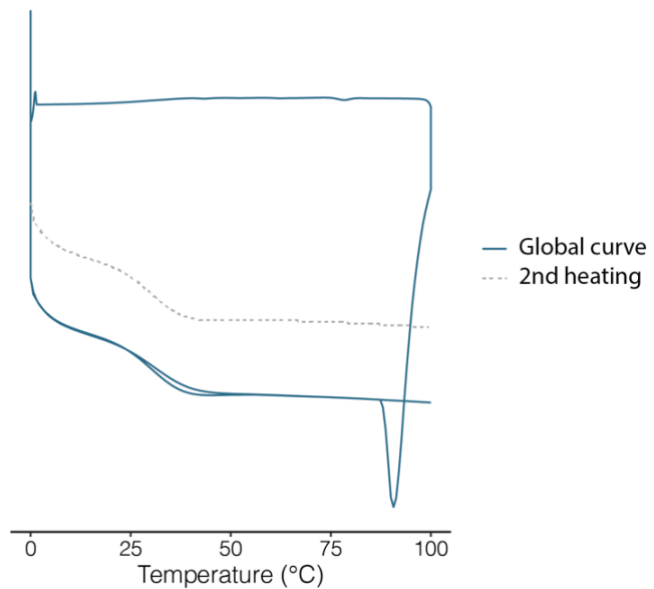


Figure S36: DSC thermogram of **PA₂-Pi** ($T_g = 30$ °C).

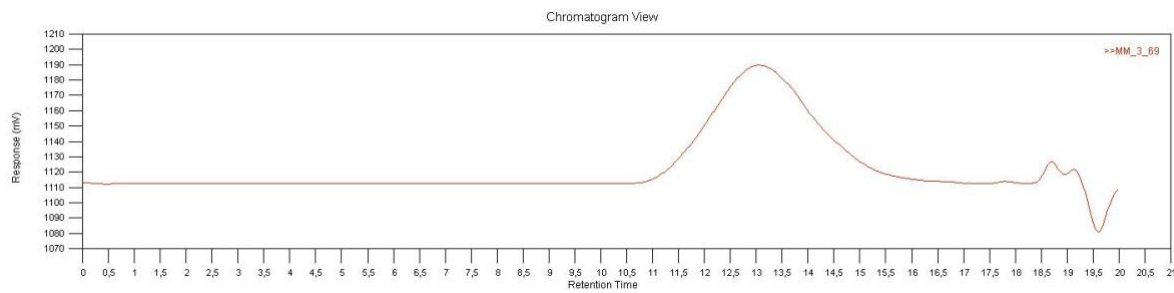


Figure S37: SEC traces of **PA₂-Pi** ($M_n = 62\,200 \text{ g/mol}$, $M_w = 148\,000 \text{ /mol}$, $D = 2.4$)

PA₂-Di

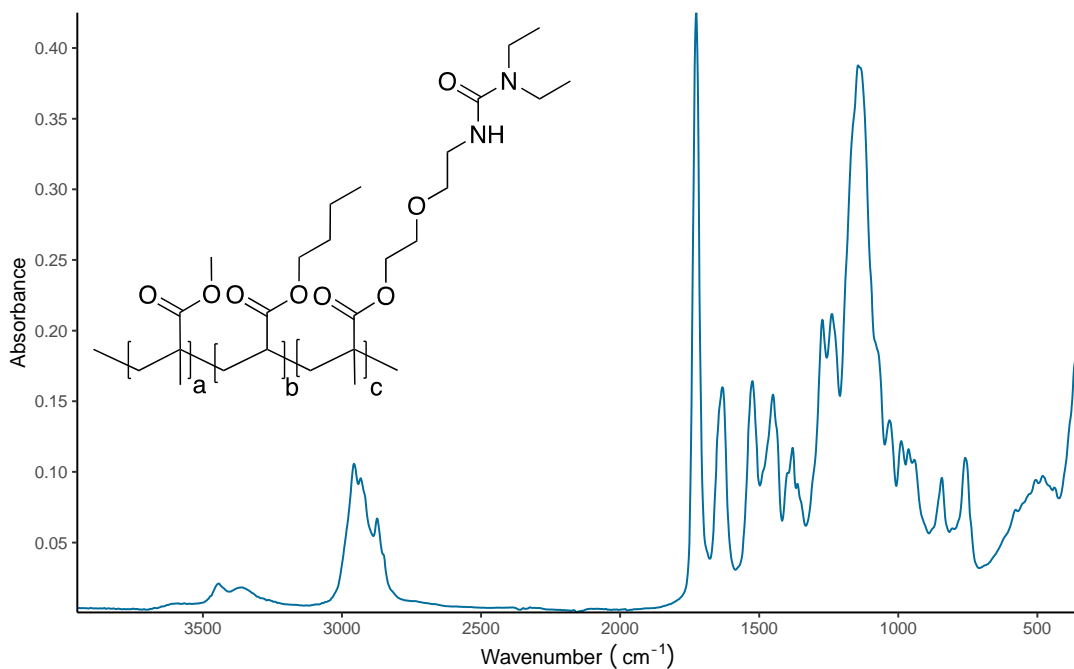


Figure S38: IR spectrum of **PA₂-Di**.

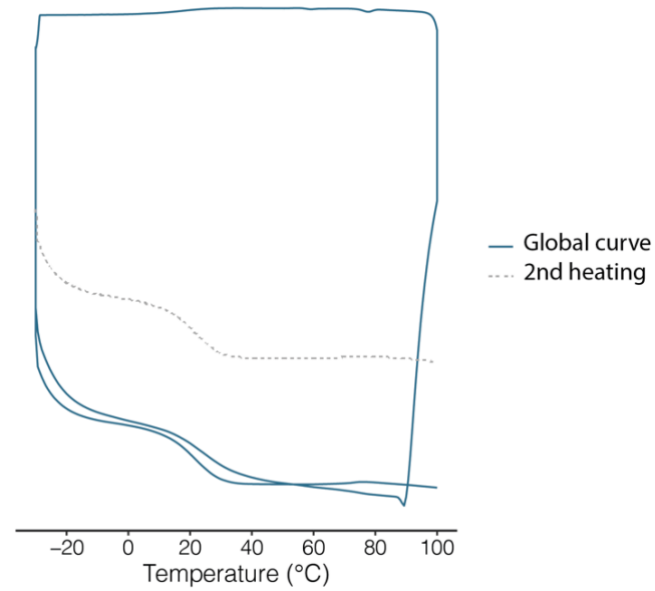


Figure S39: DSC thermogram of of **PA₂-Di** ($T_g = 16$ °C).

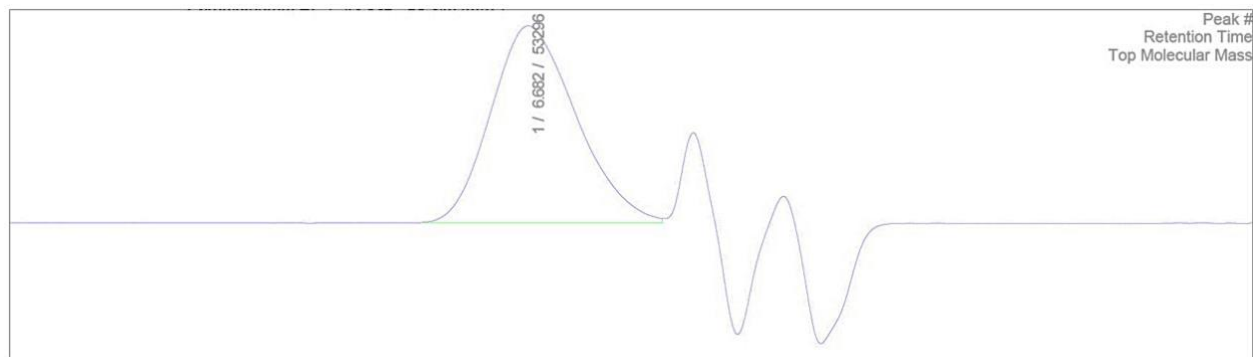


Figure S40: SEC traces of **PA₂-Di** ($M_n = 29\ 500$ g/mol, $M_w = 129\ 800$ g/mol, $D = 4.4$)

PA₂-EE

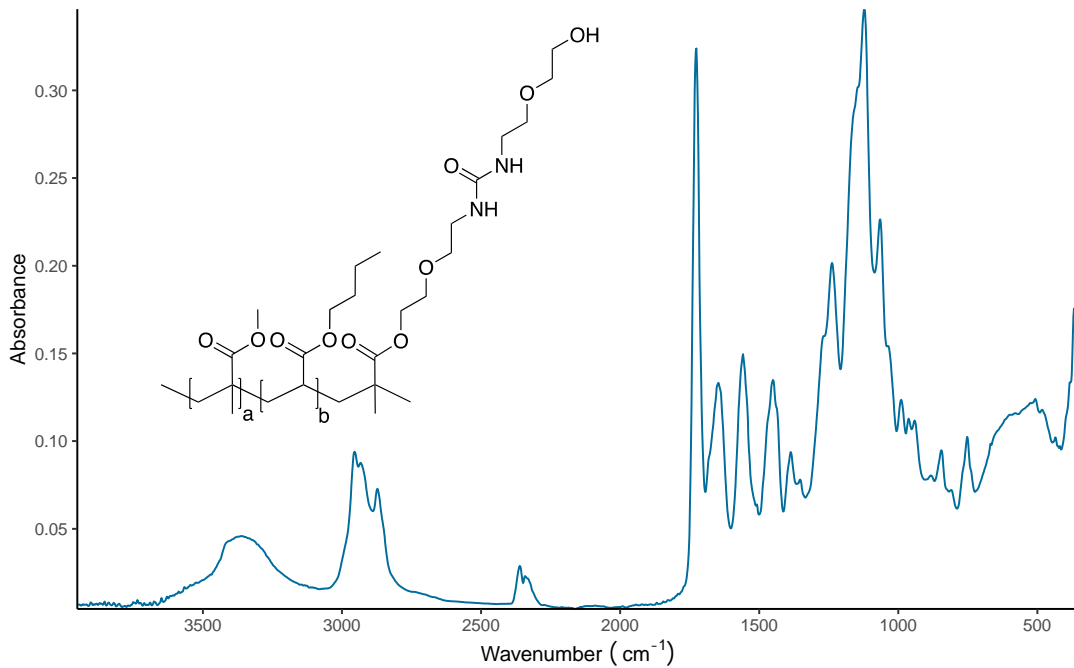


Figure S41: IR spectrum of **PA₂-EE**.

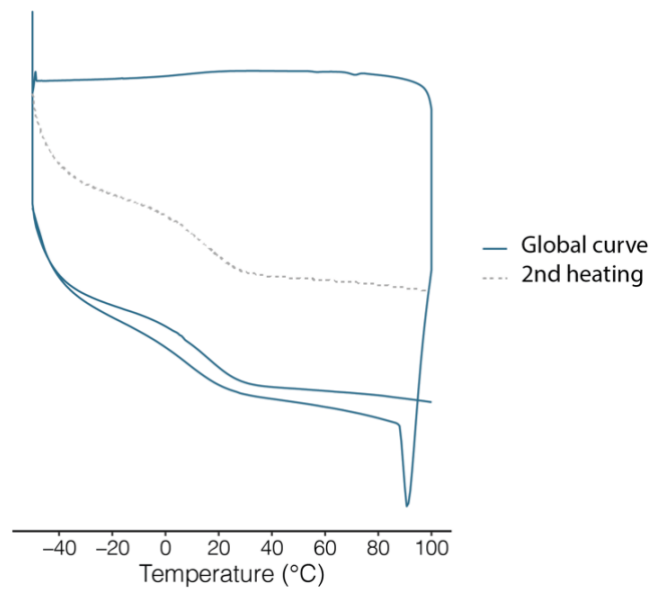


Figure S42: DSC thermogram of **PA₂-EE** ($T_g = 11$ °C).

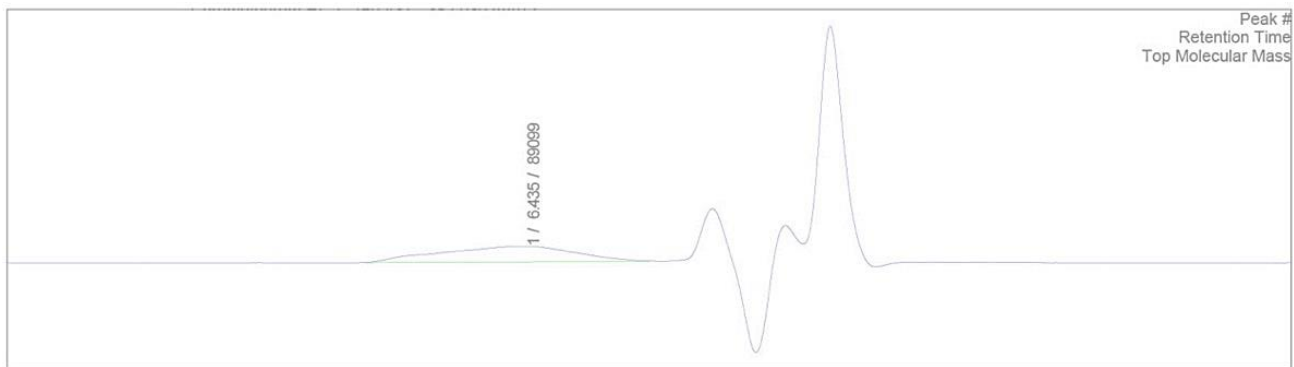


Figure S43: SEC traces of **PA₂-EE** ($M_n = 22\ 600\ g/mol$, $M_w = 100\ 600\ g/mol$, $D = 4.4$)